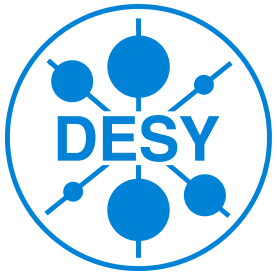

Triple differential $\frac{d^3\sigma_{\gamma,Z}}{dy_{\ell\ell}dm_{\ell\ell}d\cos\theta^*_{\mathrm{CS}}}$ cross-section measurement by ATLAS

S. Glazov
On behalf of the ATLAS collaboration
EPS 2017

Motivation for the measurement

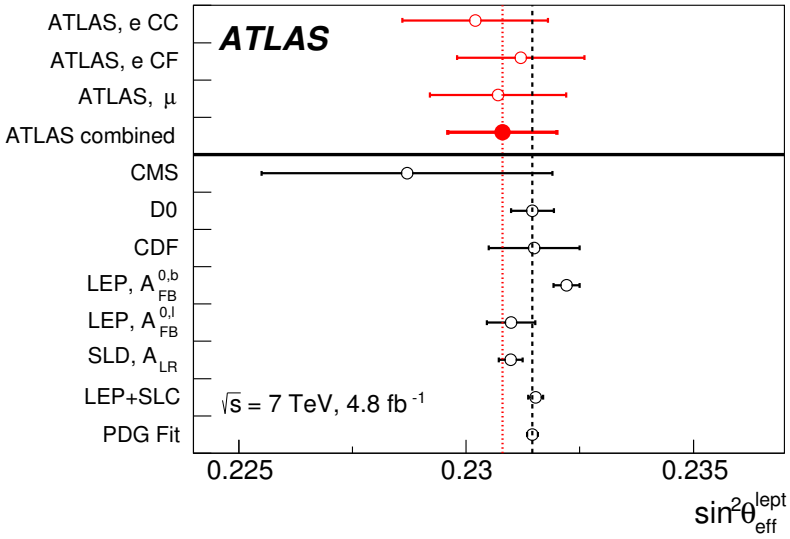

Uncertainty source	CC electrons $[10^{-4}]$	CF electrons $[10^{-4}]$	Muons $[10^{-4}]$	Combined $[10^{-4}]$
PDF	10	10	9	9
MC statistics	5	2	5	2
Electron energy scale	4	6	–	3
Electron energy resolution	4	5	–	2
Muon energy scale	–	–	5	2
Higher-order corrections	3	1	3	2
Other sources	1	1	2	2

- ATLAS measurement (JHEP09(2015)049) of $\sin^2\theta_W$ using 4.6 fb^{-1} of $\sqrt{s} = 7$ TeV data suffered from large PDF uncertainty.
- Large 20.2 fb^{-1} sample of well-understood $\sqrt{s} = 8$ TeV data.
- Design unfolded measurement to be sensitive to both PDFs and $\sin^2\theta_W$.

Introduction

$$\frac{\mathrm{d}^3\sigma}{\mathrm{d}m_{\ell\ell}\mathrm{d}y_{\ell\ell}\mathrm{d}\cos\theta^*_{\mathrm{CS}}} = \frac{\pi\alpha^2}{3m_{\ell\ell}s}\sum_q P_q\left[f_q(x_1,Q^2)f_{\bar{q}}(x_2,Q^2) + (q \leftrightarrow \bar{q})\right],$$

$$\cos\theta^*_{\mathrm{CS}} = \frac{p_{\mathrm{z},\ell\ell}}{m_{\ell\ell}|p_{\mathrm{z},\ell\ell}|}\frac{p_1^+p_2^- - p_1^-p_2^+}{\sqrt{m_{\ell\ell}^2 + p_{\mathrm{T},\ell\ell}^2}}\,.$$

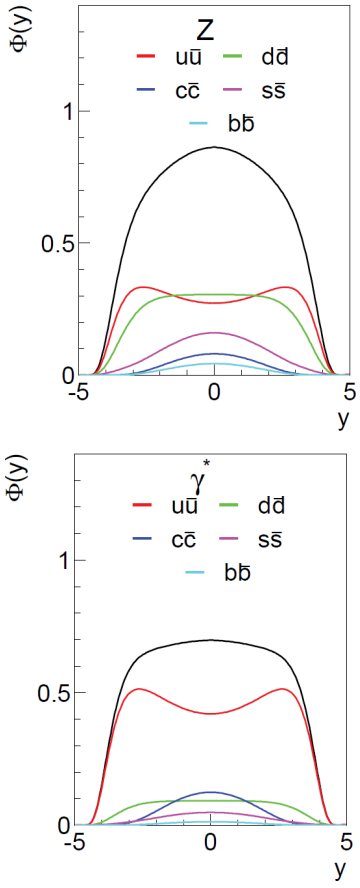

- The Z/γ^* differential cross section is a product of PDFs and propagator terms. Difference in couplings allows for PDF decomposition.
- Terms proportional to Z and γ^* contribute differently at different $m_{\ell\ell}$.
- Interference term generates $\cos\theta^*_{\mathrm{CS}}$ asymmetry which changes sign at M_Z. The asymmetry vanishes at $y_{\ell\ell} = 0$, and increases with $y_{\ell\ell}$, due to larger difference in q and $\bar{q}$ contributions.

→ Triple differential measurement in $m_{\ell\ell}, y_{\ell\ell}, \cos\theta^*_{\mathrm{CS}}$, with one of the bin boundaries at M_Z.

The measurement

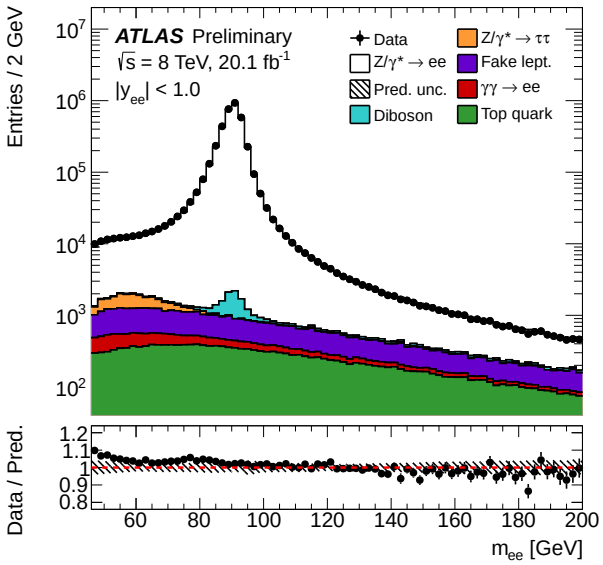

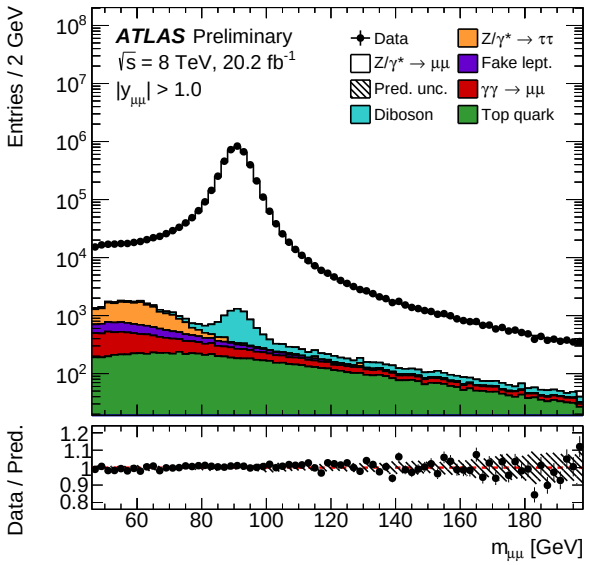

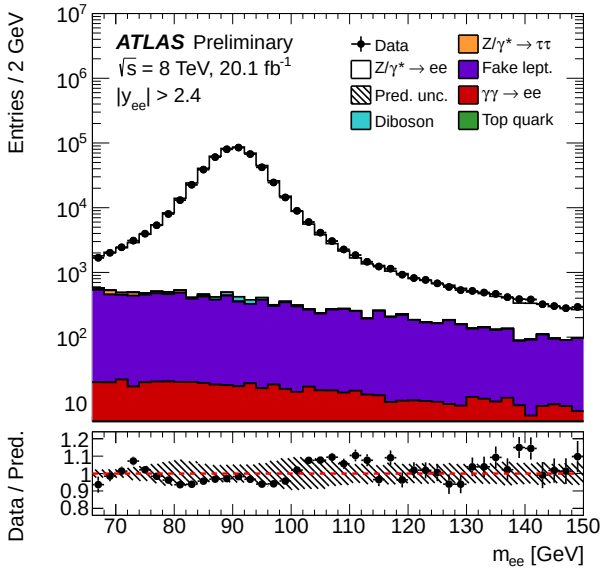

- Measurement using central $|\eta^{\ell}| < 2.4$, $p_T^{\ell} > 20$ GeV electrons and muons, in seven $46 < m_{\ell\ell} < 200$ GeV, twelve $y_{\ell\ell} < 2.4$ and six $\cos\theta^*_{\mathrm{CS}}$ bins (2×504 bins in total).
- Measurement using one central (with p_T cut increased to 25 GeV) and one forward electron $|\eta^{\ell}| > 2.5$, $p_T^{\ell} > 20$ GeV in five $66 < m_{\ell\ell} < 150$, five $1.2 < y_{\ell\ell} < 3.6$ and six $\cos\theta^*_{\mathrm{CS}}$ bins (150 bins in total).
- Drell-Yan signal MC uses Powheg with CT10 PDF set, with mass-dependent NNLO/NLO k-factor and $p_{\mathrm{T}}^{\ell\ell}$-dependent polarisation coefficients correction computed using DYNNLO. .

$\cos\theta^*_{\mathrm{CS}}$ at the Z-peak

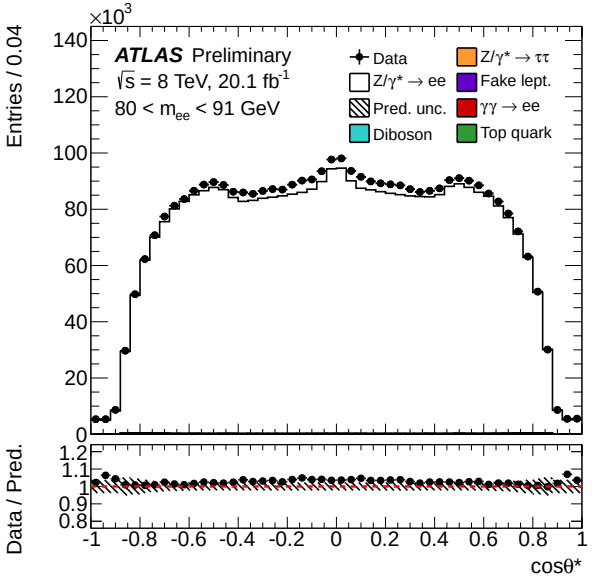

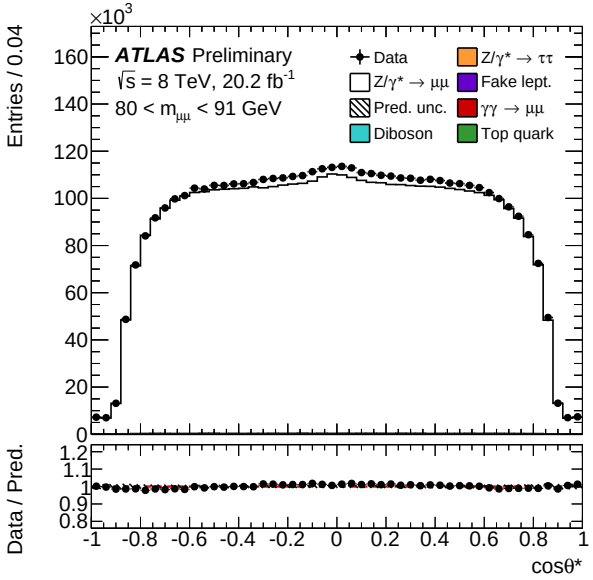

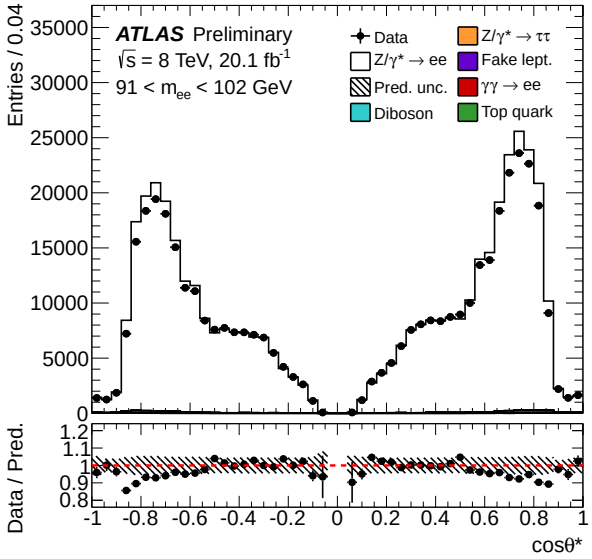

- Bins under the Z-boson peak ($80 < m_{\ell\ell} < 91$ GeV and $91 < m_{\ell\ell} < 102$ GeV) are symmetric in $\cos\theta^*_{\mathrm{CS}}$ and almost background free for both central-central (CC) and central forward (CF) toplogies.
- CF analysis allows to extend results not only in $y_{\ell\ell}$ but also probes larger $\cos\theta^*_{\mathrm{CS}}$.
- Main systematic sources for the peak region are efficiencies ($< 0.5\%$), energy scale and resolution ($\sim 1\%$), and charge-dependent momentum reconstruction for muons, affected by alignment weak modes ($\sim 1\%$).

$\cos\theta^*_{\mathrm{CS}}$ above the Z-peak

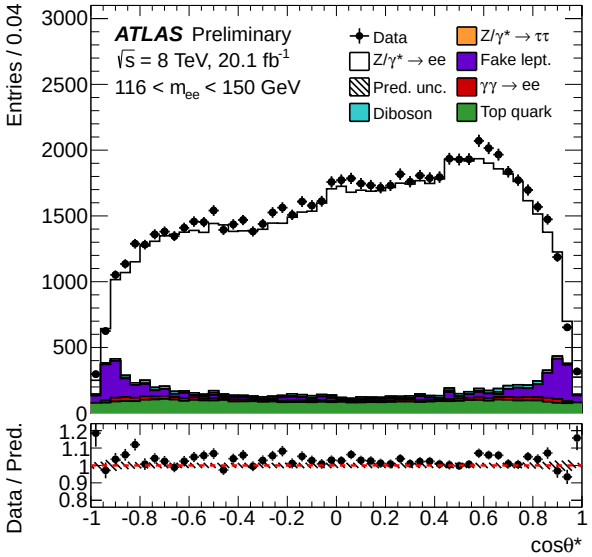

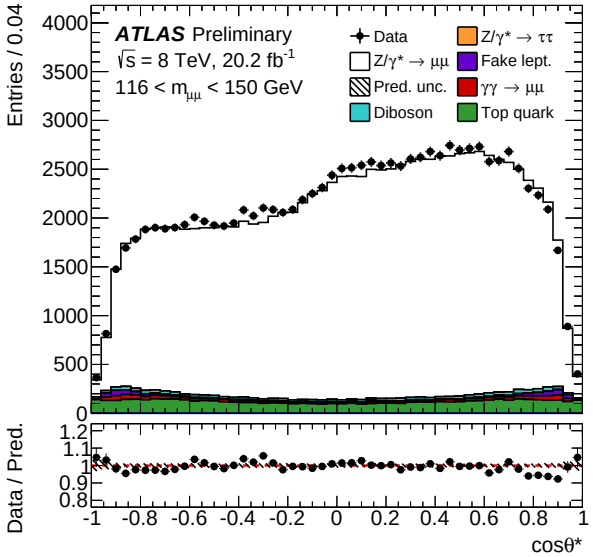

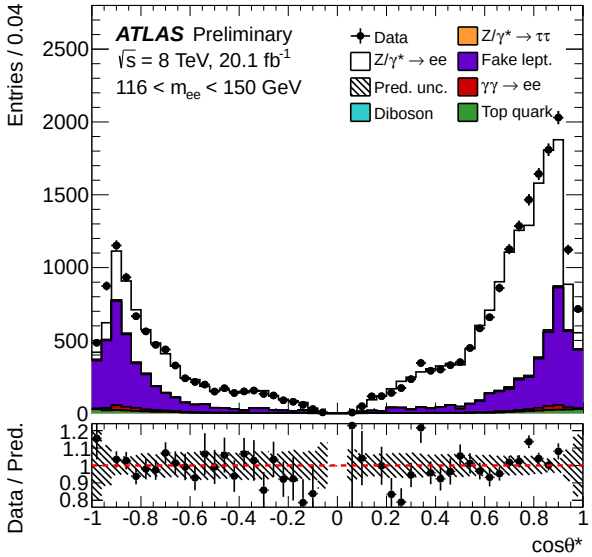

- For $m_{\ell\ell}$ above the Z-peak, FB asymmetry develops.
- Backgrounds from top quark and multijet production become sizable, for CF topology in particular. Most of backgrounds (apart for W+jets) are charge symmetric and do not affect the FB asymmetry.
- Leading systematic sources are from background subtraction, and also forward energy resolution (for CF topology).

Single differential $d\sigma/dm_{\ell\ell}$ cross section

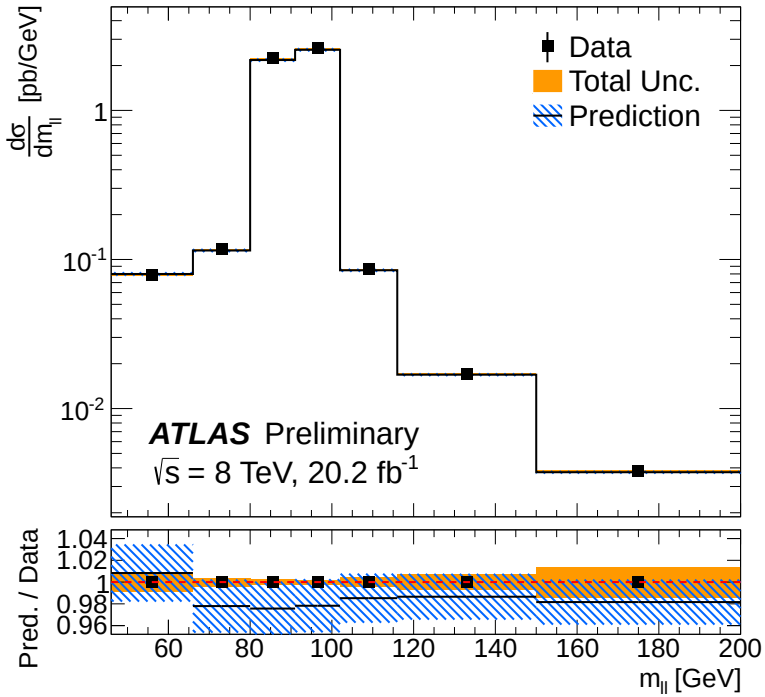

- Unfolded 3D cross sections measured in electron and muon CC channels can be integrated to 1D and 2D and compared to each other. For $d\sigma/dm_{\ell\ell}$, combination $\chi^2/N_{\mathrm{DF}} = 12.8/7$.
- Cross section can be first combined and then integrated. Comparison with the Powheg-based prediction shows good agreement overall.

Double differential $d^2\sigma/dm_{\ell\ell}dy_{\ell\ell}$ cross section

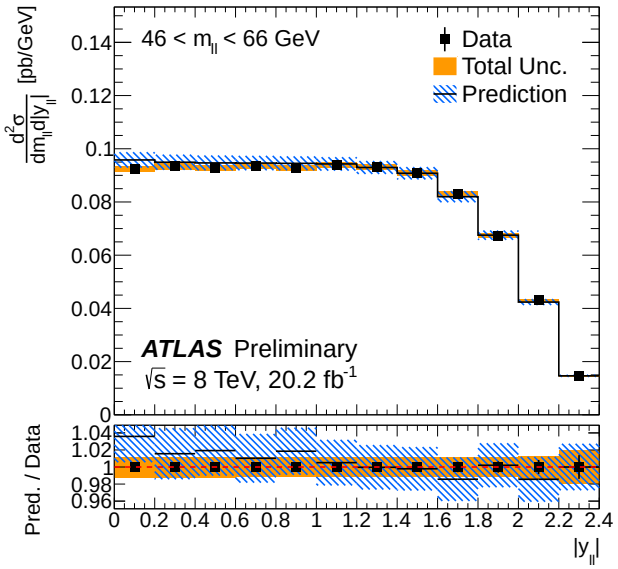

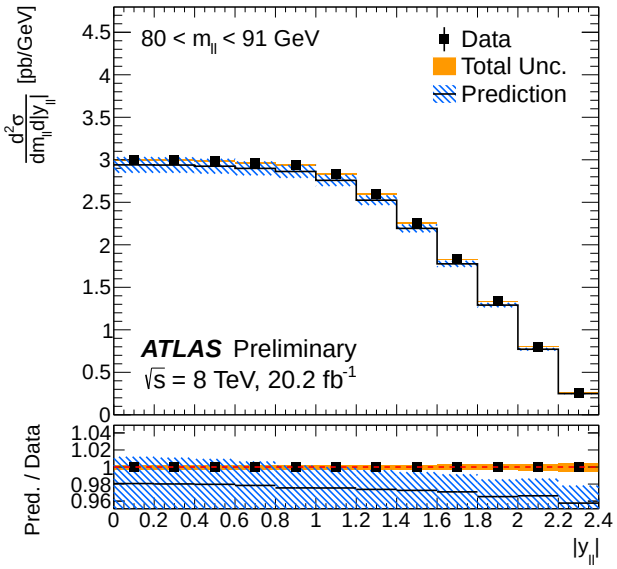

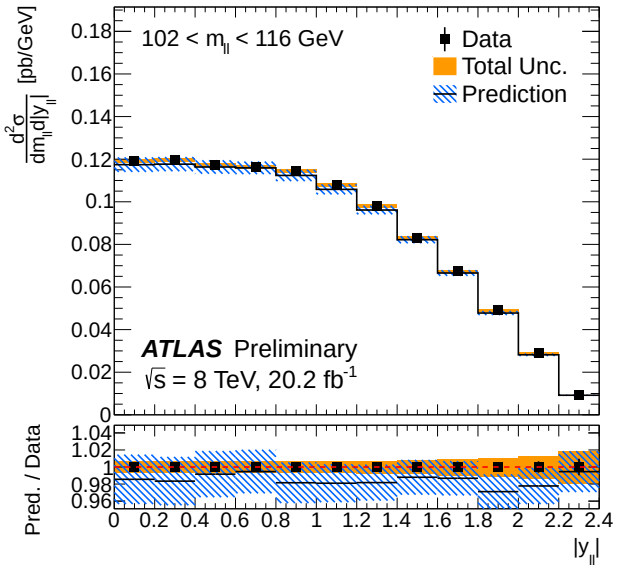

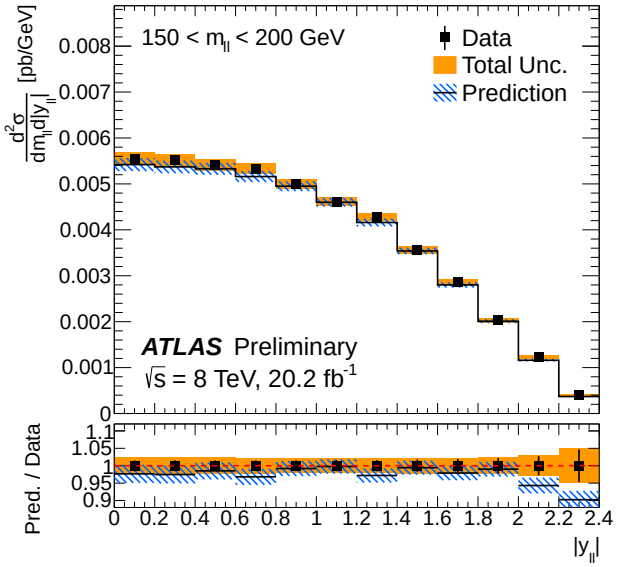

- Similarly, cross sections can be integrated to two-dimensions.
- Electron and muon channels agree well with $\chi^2/N_{\mathrm{DF}} = 103.4/84$.
- The comparison with Powheg-based predictions are good overall.

Triple differential cross section I

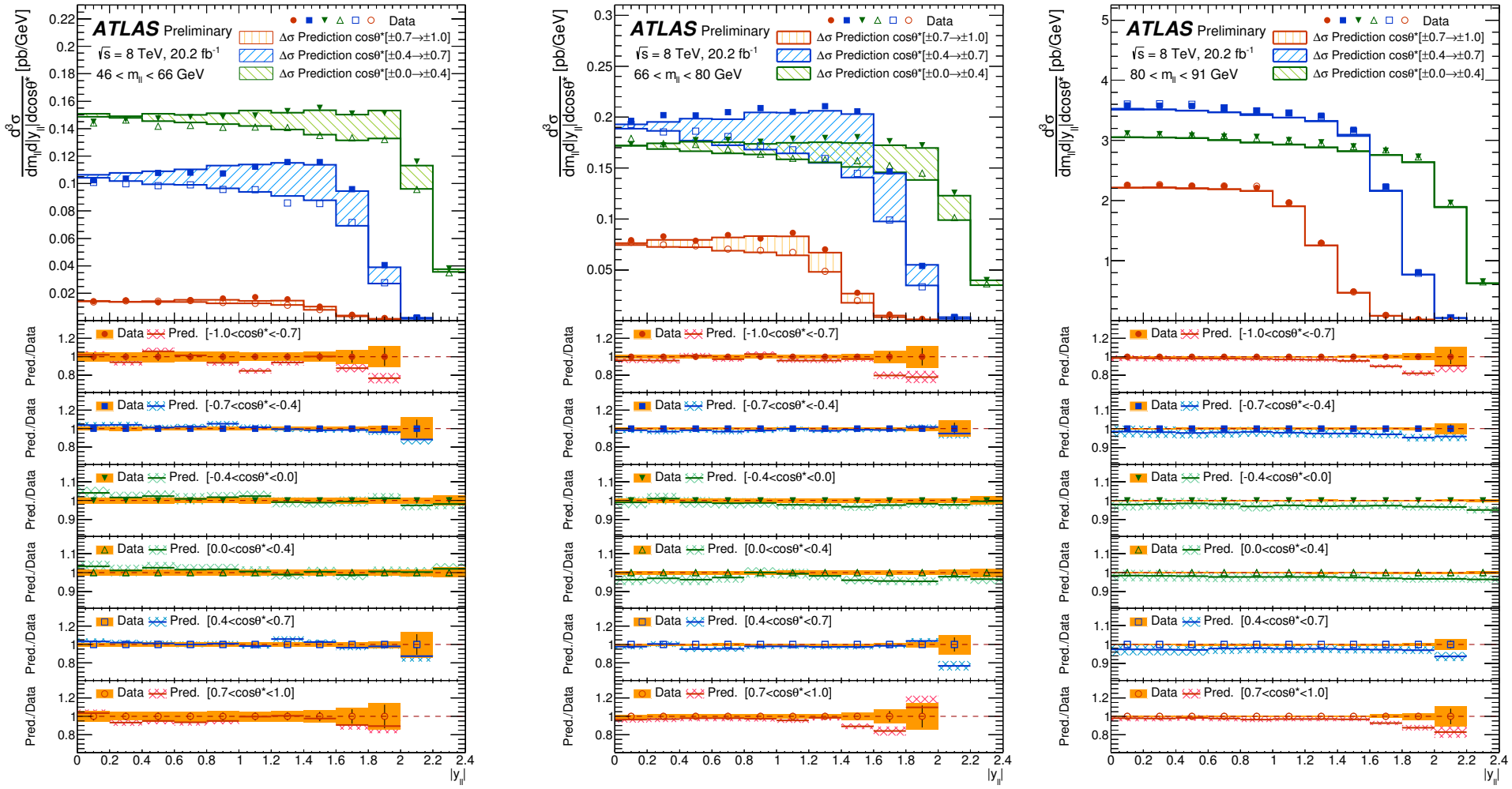

- Negative FB-asymmetry below the Z-peak, vanishing at the peak.
- Increasing with mass cross section for large $\cos\theta^*_{\mathrm{CS}}$ due to reduced impact of fiducial cuts.

Triple differential cross section II

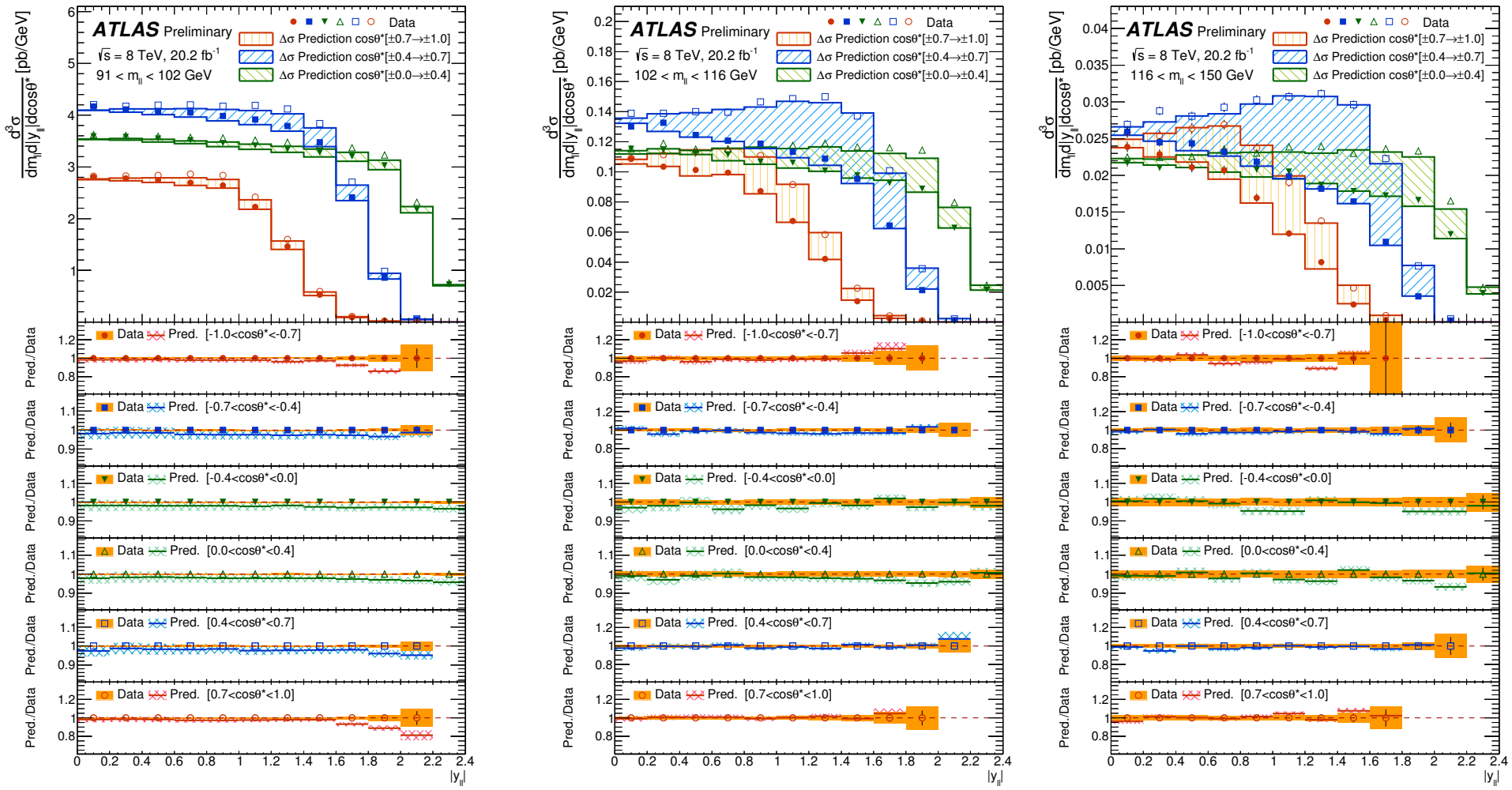

- The asymmetry flips sign above Z-peak and increases towards larger $m_{\ell\ell}$.

Triple differential cross section III

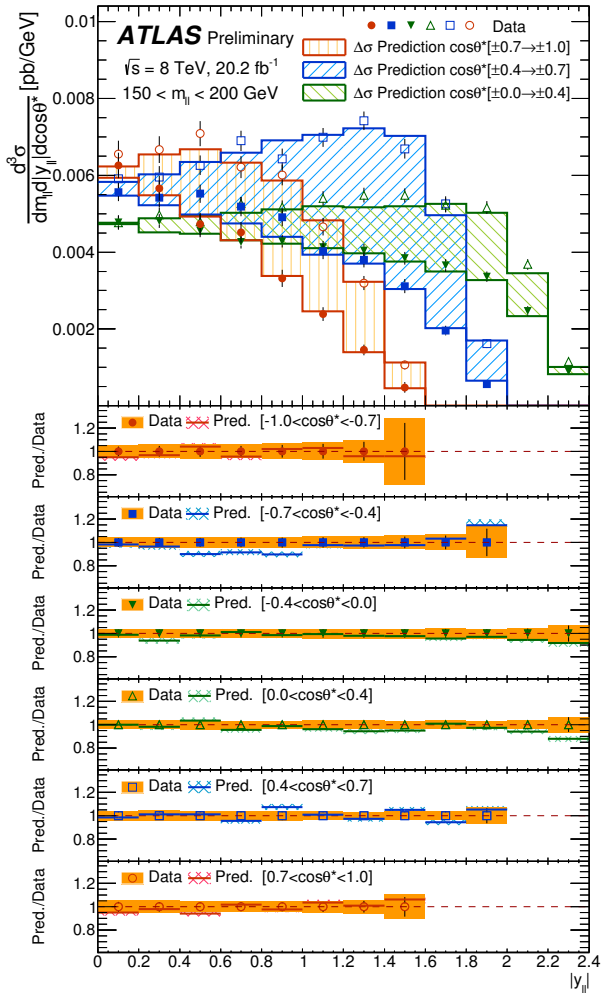

- Combination of electron and muon channels yield good $\chi^2/N_{\mathrm{DF}} = 489.4/451$.
- The data accuracy is better than 0.5% in the Z-peak region for $|y_{\ell\ell}| < 1.4$.
- Overall good agreement between data and Powheg-based predictions.

Example results of central-forward analysis

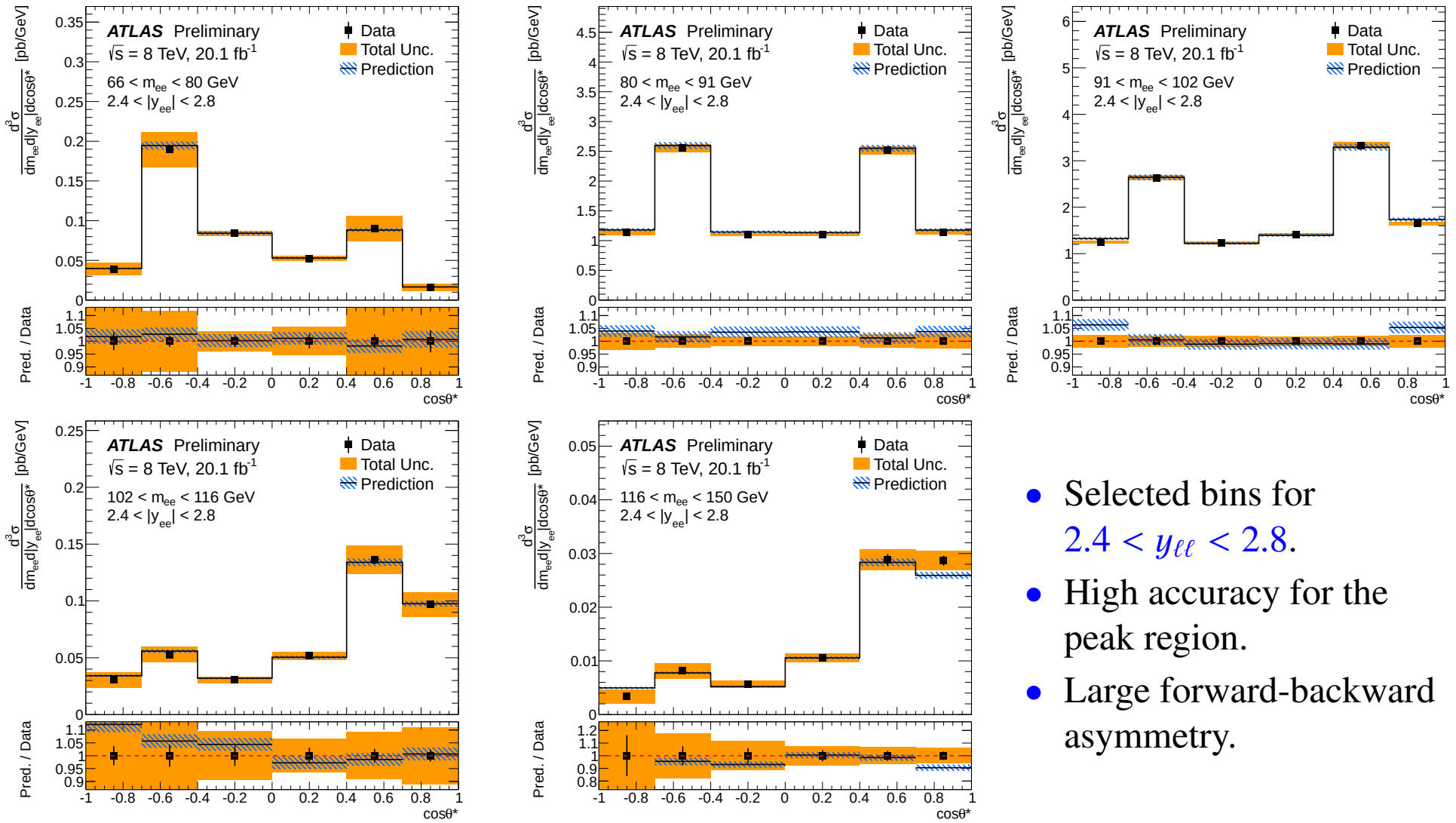

- Selected bins for $2.4 < y_{\ell\ell} < 2.8$.
- High accuracy for the peak region.
- Large forward-backward asymmetry.

→ Powheg describes data well.

Forward-backward asymmetry: Combined Central

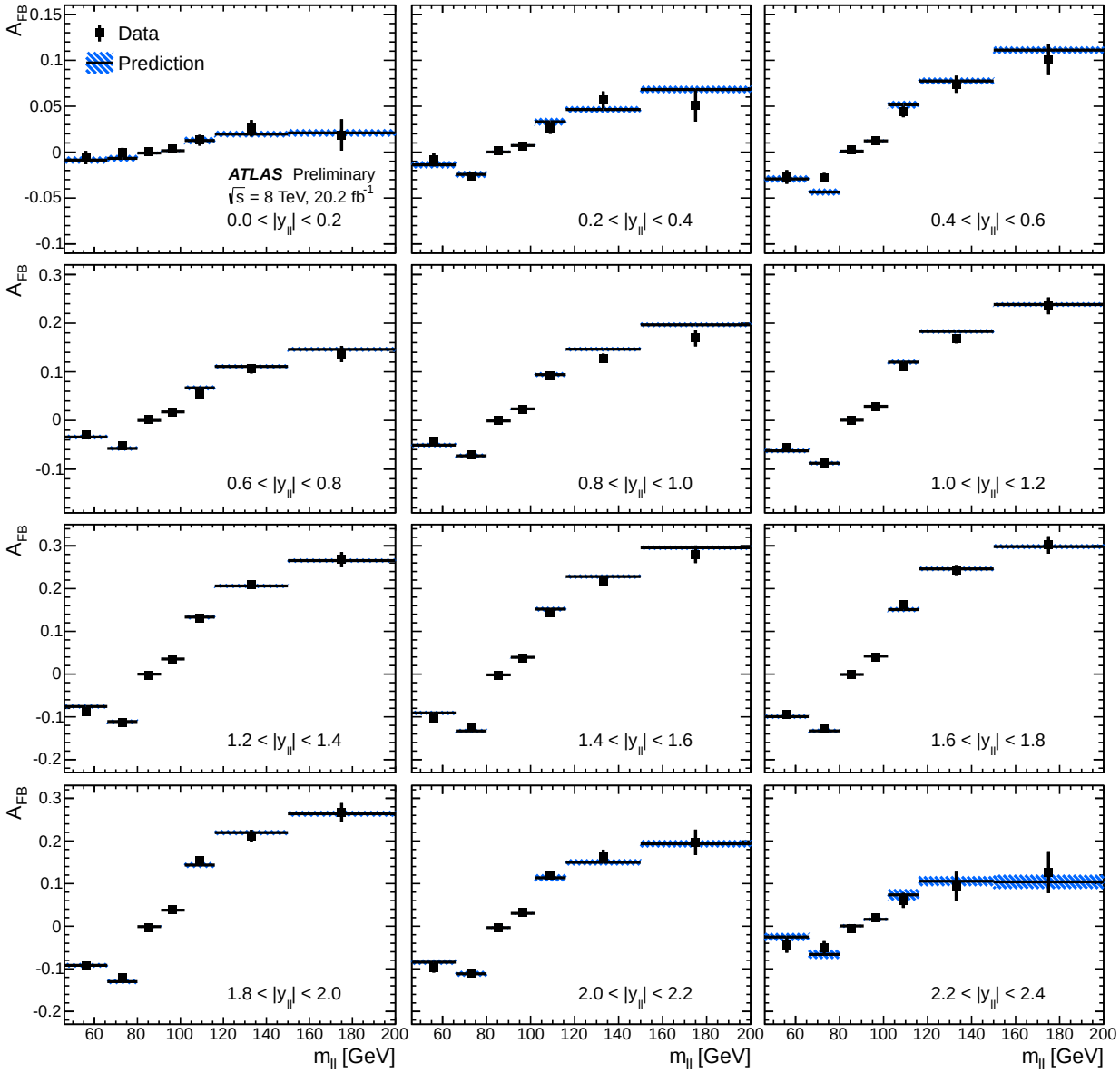

Compute

$$A_{\mathrm{FB}} = \frac{\mathrm{d}^3\sigma(\cos\theta^* > 0) - \mathrm{d}^3\sigma(\cos\theta^* < 0)}{\mathrm{d}^3\sigma(\cos\theta^* > 0) + \mathrm{d}^3\sigma(\cos\theta^* < 0)}$$

- Uncertainties symmetric in $\cos\theta_{CS}$, such as scale and resolution, cancel.
- Asymmetry increases in $y_{\ell\ell}$ due to reduced dilution, when levels off and drops for last bins due to fiducial acceptance.
- Good agreement with the CT10-based Powheg prediction.

Forward-backward asymmetry: Central Forward

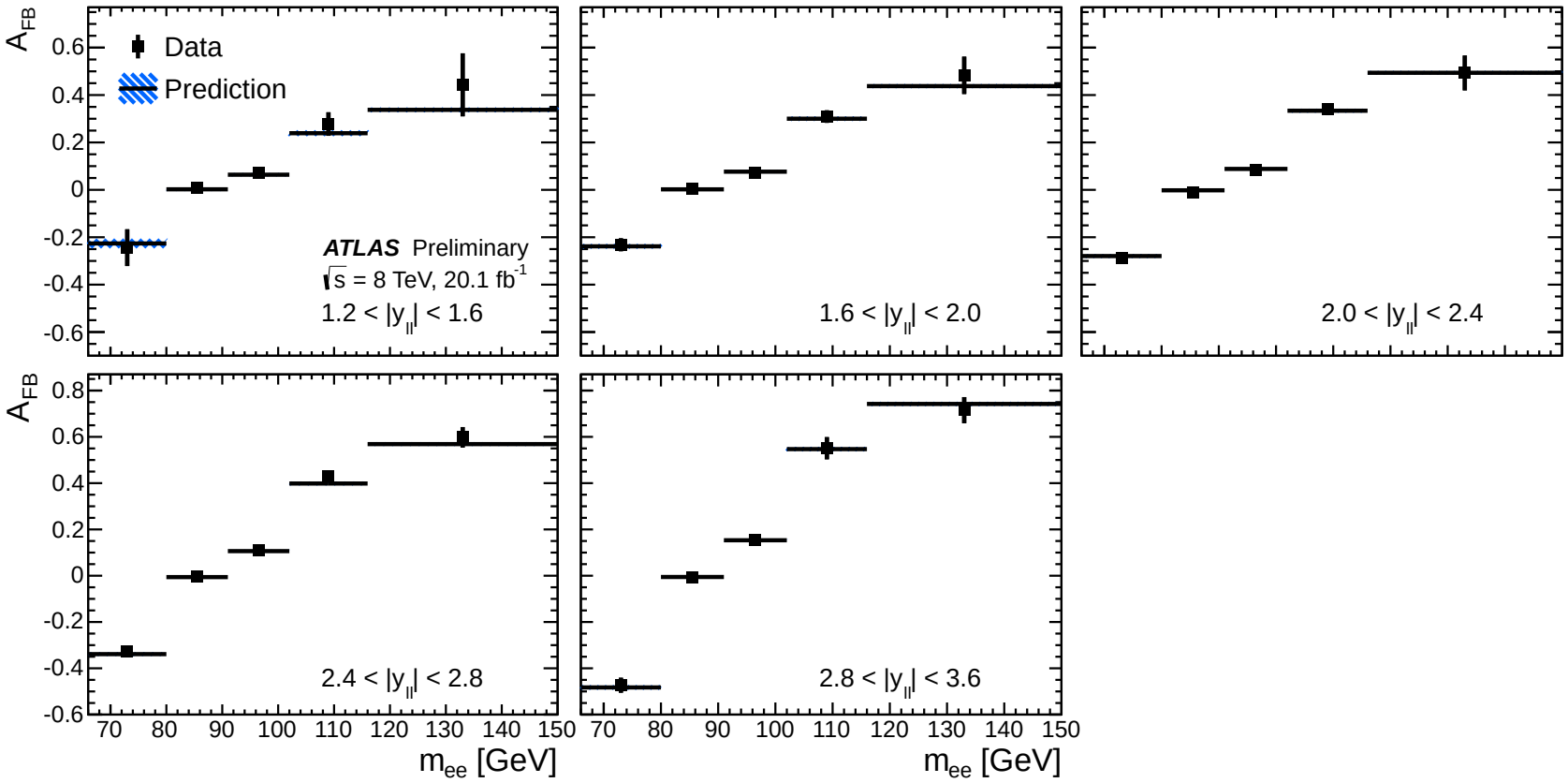

- Cancellation of $\cos\theta^*_{CS}$ symmetric uncertainties is even more important for CF analysis.
- Measured A_{FB} ranges from -0.2 to +0.5 at the lowest and from -0.4 to +0.7 at the highest $y_{\ell\ell}$, in agreement with predictions.

Measurement of τ polarisation in Z/γ^* decays

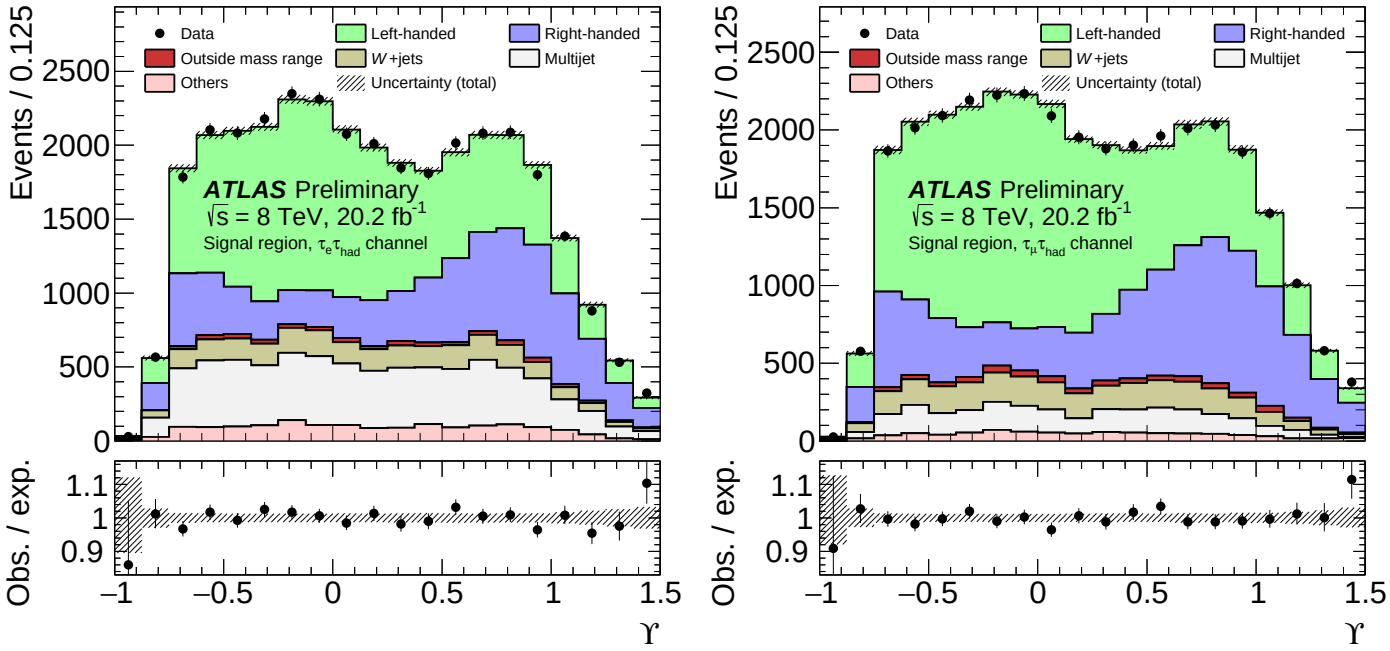

- Measurement of the τ polarisation in Z/γ^* decays using leptonic plus single-prong hadronic τ decay, based on $\sqrt{s} = 8$ TeV data.
- Polarisation is determined from the ratio of charged to neutral energy in hadronic decays, estimated as $\Upsilon = 2\frac{p_{\mathrm{T}}^{\mathrm{track}}}{E_{\mathrm{T}}^{\tau}} - 1$
- Fiducial results are extrapolated to $66 < M_{\tau\tau} < 116$ GeV mass range to give $P_\tau = -0.14 \pm 0.02\ \mathrm{stat} \pm 0.04\ \mathrm{syst}$ in agreement with the expectation $P_\tau = -0.1517 \pm 0.0019$ based on ALPGEN+Pythia6+Tauola.

ATLAS-CONF-2017-049.

Summary

- Unique measurement of the triple differential $\frac{d^3\sigma_{\gamma,Z}}{dy_{\ell\ell}dm_{\ell\ell}d\cos\theta^*_{\rm CS}}$ cross section in a wide kinematic range, $46 < m_{\ell\ell} < 200$ GeV and $y_{\ell\ell} < 3.6$, using $\sqrt{s} = 8$ TeV ATLAS data.
- The measurement is designed to be sensitive to both PDFs and $\sin^2\theta_W$.
- In the Z-peak region, the data accuracy is better than 0.5% in a wide region of $|y_{\ell\ell}| < 1.4$.
- The measurement is used to compute single- and double-differential $d\sigma/dm_{\ell\ell}$ and $d^2\sigma/dm_{\ell\ell}dy_{\ell\ell}$ cross sections as well as forward-backward asymmetry.
- The results are well described by modified Powheg predictions.
- New measurements of τ polarisation in Z/γ^* decays agrees well with the expectations.

Results of central-forward analysis

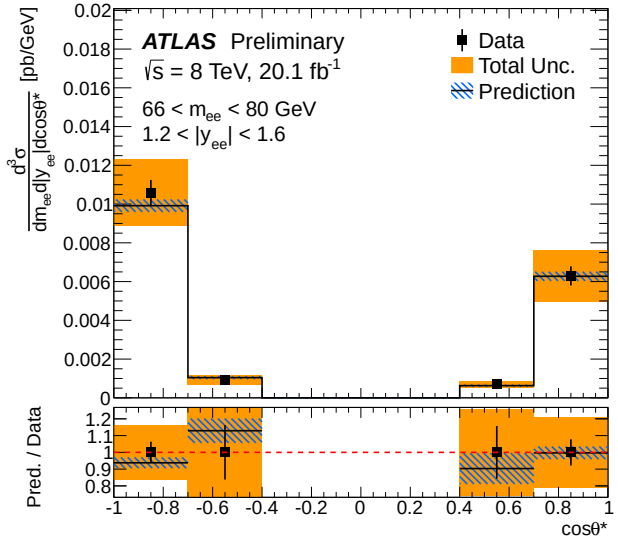

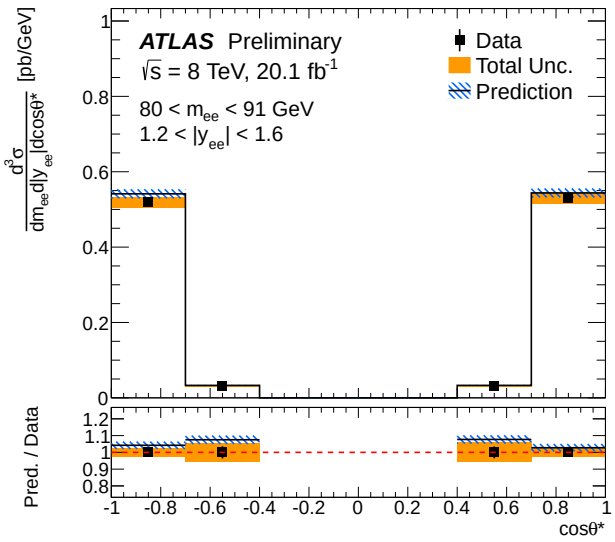

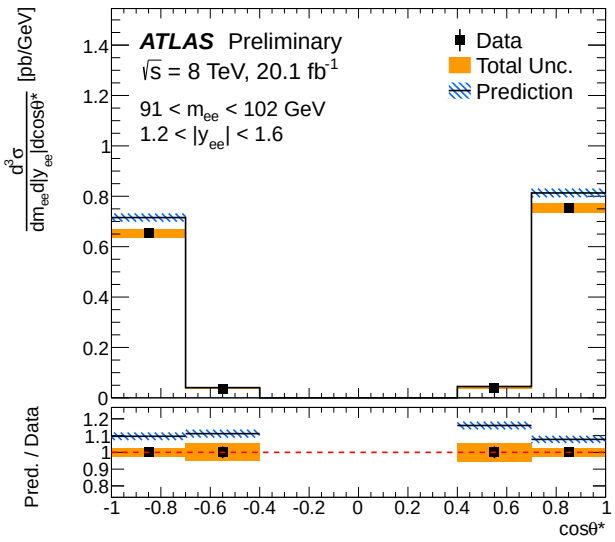

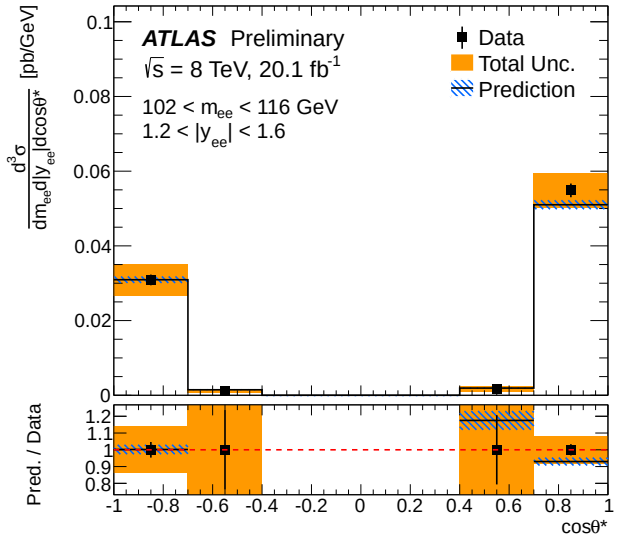

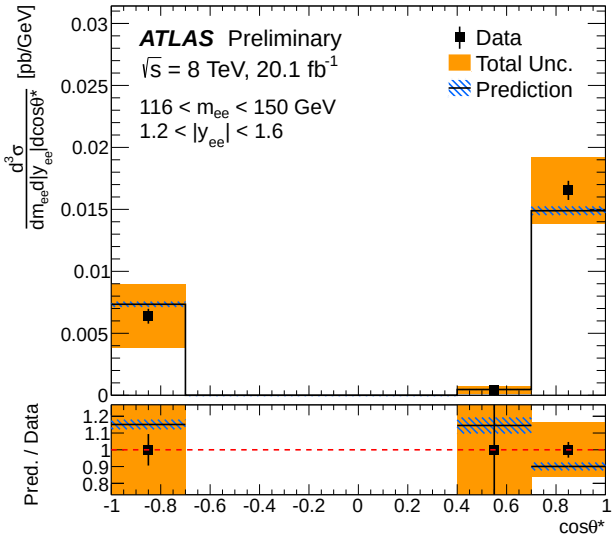

- Bins for $1.2 < y_{\ell\ell} < 1.6$.
- High accuracy for the peak region.
- Large forward-backward asymmetry.

→ Powheg describes data well.

Results of central-forward analysis

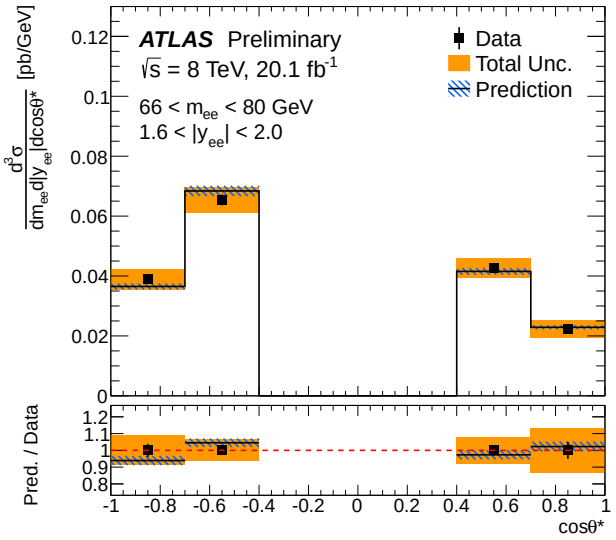

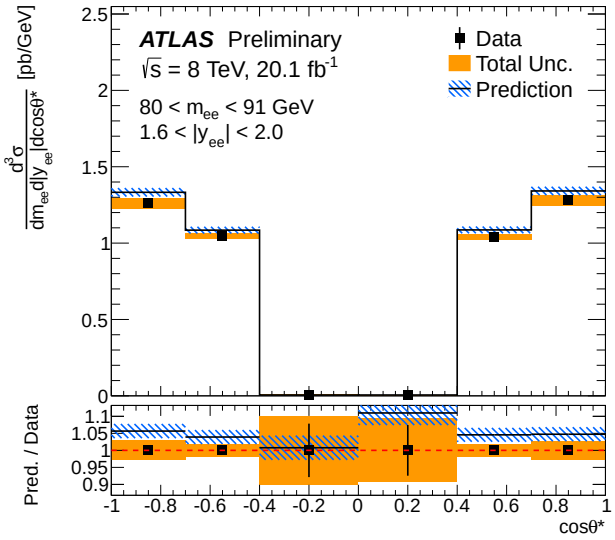

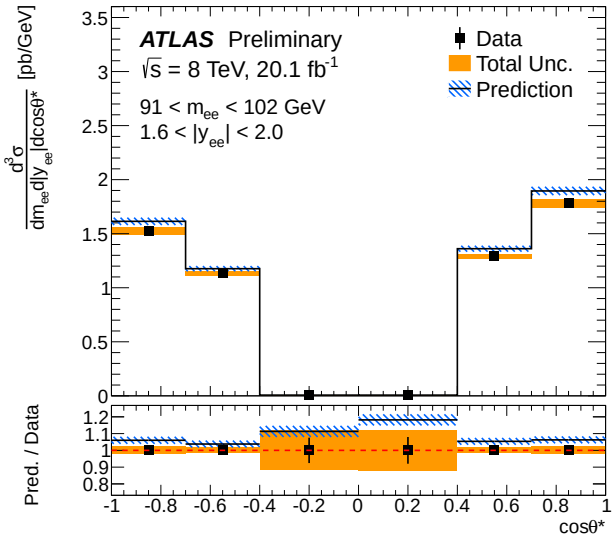

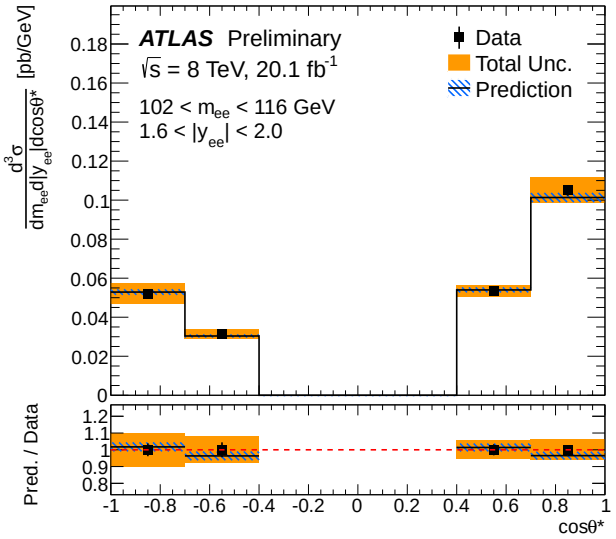

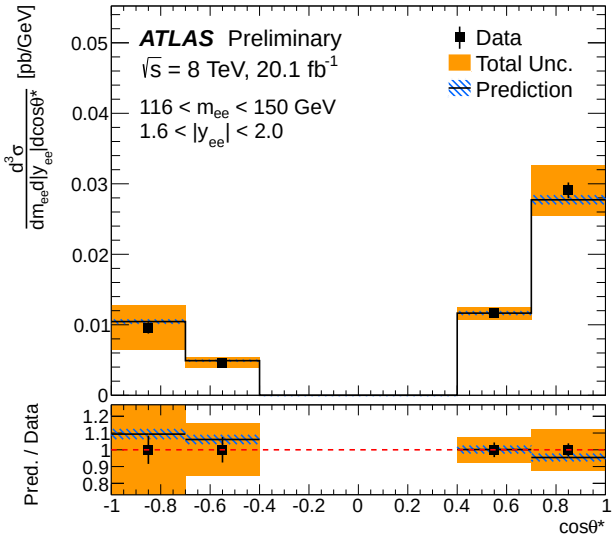

- Bins for $1.6 < y_{\ell\ell} < 2.0$.
- High accuracy for the peak region.
- Large forward-backward asymmetry.

→ Powheg describes data well.

Results of central-forward analysis

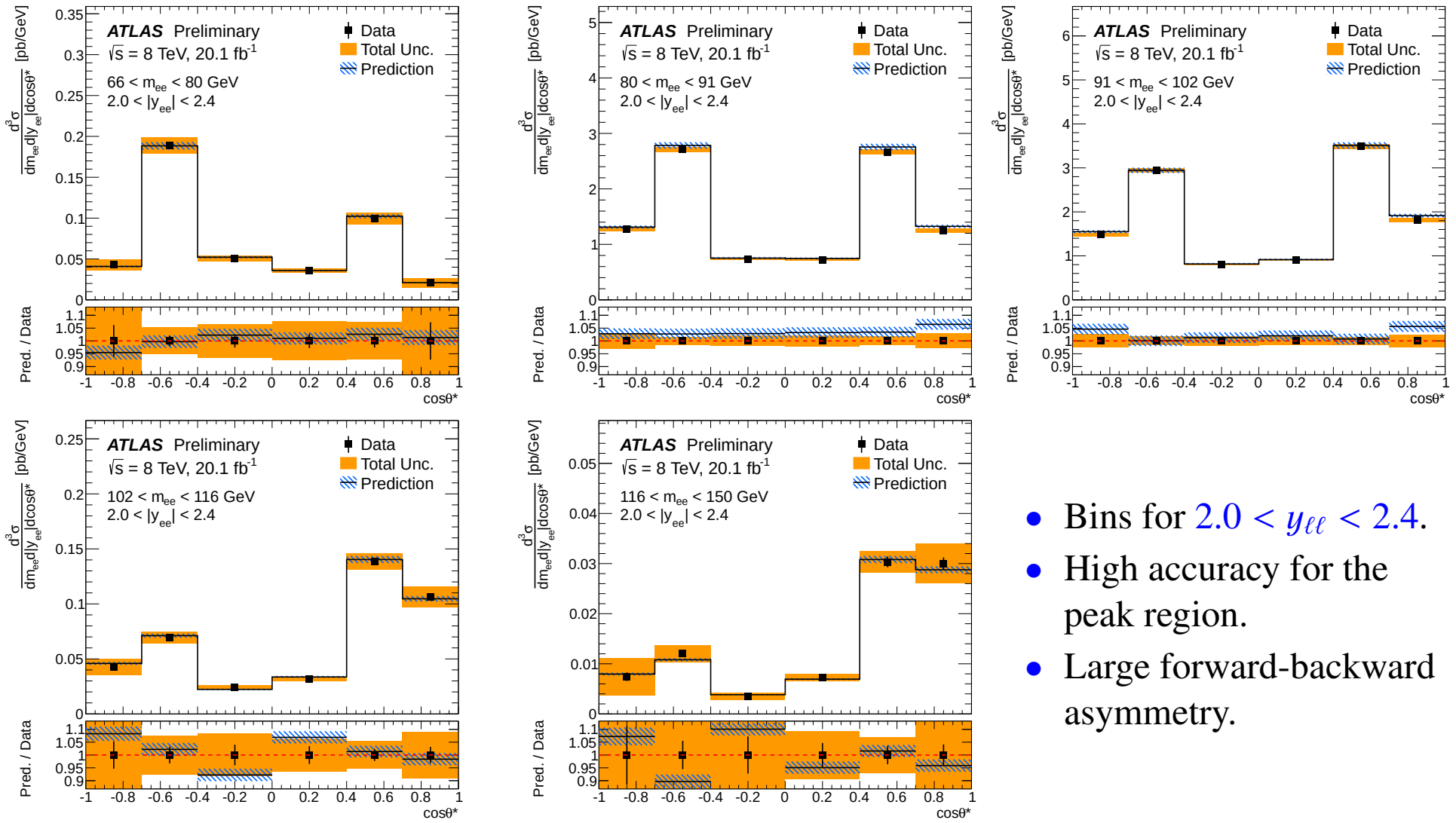

- Bins for $2.0 < y_{\ell\ell} < 2.4$.
- High accuracy for the peak region.
- Large forward-backward asymmetry.

→ Powheg describes data well.

Results of central-forward analysis

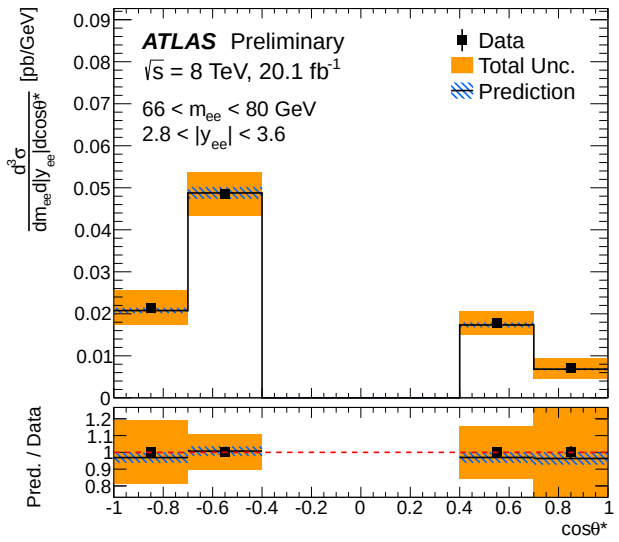

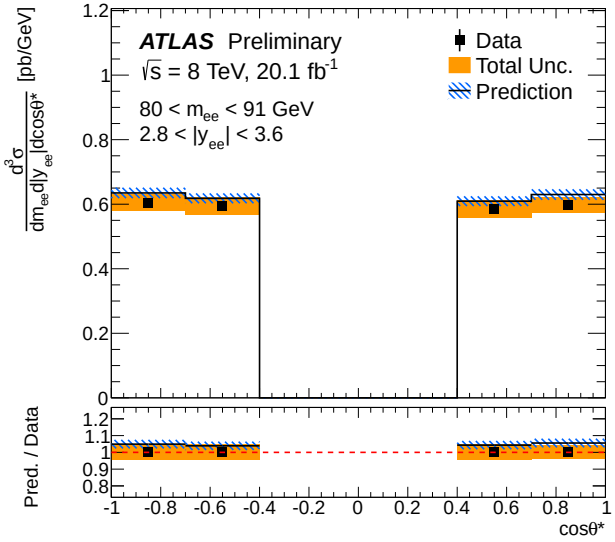

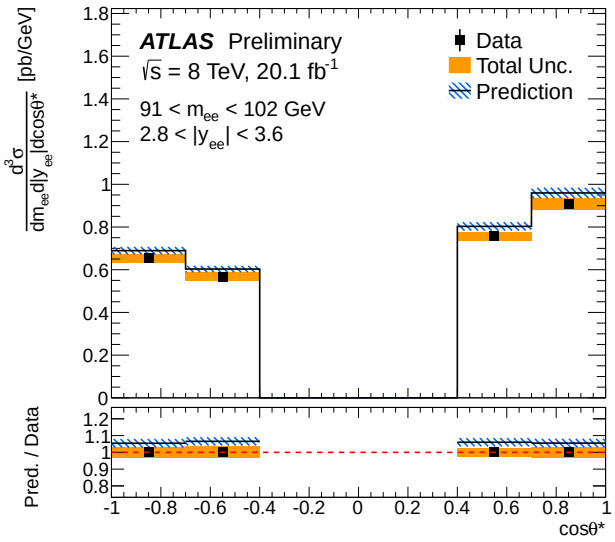

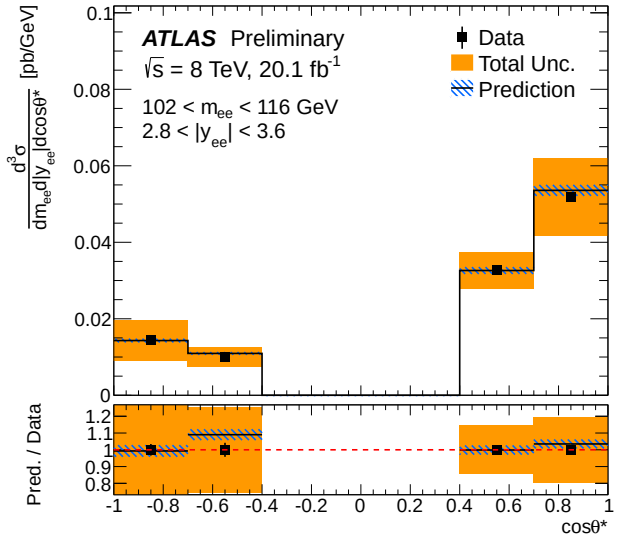

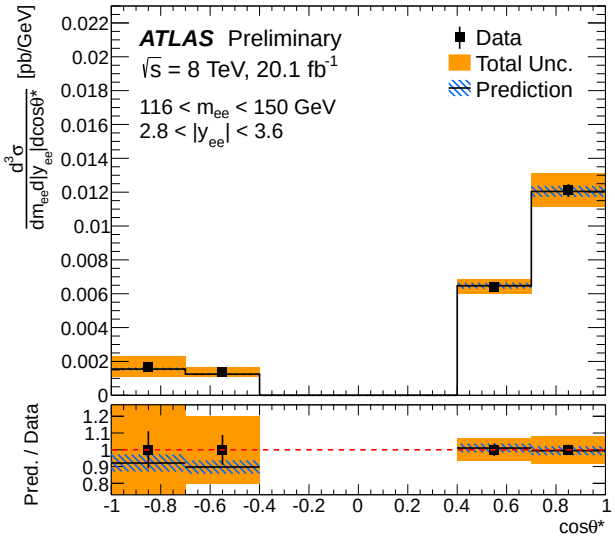

→ Powheg describes data well.

- Bins for $2.8 < y_{\ell\ell} < 3.6$.
- High accuracy for the peak region.
- Large forward-backward asymmetry.

Cross section decomposition

$$P_q = e_l^2 e_q^2 (1 + \cos^2\theta^*)$$
$$+ e_l e_q \frac{2m_{\ell\ell}^2 (m_{\ell\ell}^2 - m_Z^2)}{\sin^2\theta_W \cos^2\theta_W [(m_{\ell\ell}^2 - m_Z^2)^2 + \Gamma_Z^2 m_Z^2]} [v_\ell v_q (1 + \cos^2\theta^*) + 2a_\ell a_q \cos\theta^*]$$
$$+ \frac{m_{\ell\ell}^4}{\sin^4\theta_W \cos^4\theta_W [(m_{\ell\ell}^2 - m_Z^2)^2 + \Gamma_Z^2 m_Z^2]} [(a_\ell^2 + v_\ell^2)(a_q^2 + v_q^2)(1 + \cos^2\theta^*) + 8a_\ell v_\ell a_q v_q \cos\theta^*].$$